

Application of Gold Nanoparticle and Three-Dimensional Graphene Based Electrode for Sensitive Voltammetric Analysis of Luteolin

Zuorui Wen¹, Xiaoyan Li¹, Xueliang Niu¹, Wenshu Zhao¹, Yong Cheng², Qianwen Ma¹, Xiaobao Li¹, Wei Sun^{1,*}, Guangjiu Li²

¹ Key Laboratory of Tropical Medicinal Plant Chemistry of Ministry of Education, College of Chemistry and Chemical Engineering, Hainan Normal University, Haikou 571158, P R China,

² College of Chemistry and Molecular Engineering, Qingdao University of Science and Technology, Qingdao 266042, P. R. China

*E-mail: swyy26@hotmail.com

Received: 20 February 2017 / Accepted: 29 March 2017 / Published: 12 May 2017

A nanocomposite composed of gold nanoparticle (Au) and three-dimensional graphene (3DGR) was electrodeposited on the surface of carbon ionic liquid electrode (CILE), which exhibited synergistic effects with improved electrochemical performance. Voltammetric behaviors of luteolin on Au/3DGR/CILE were evaluated with the electrochemical parameters calculated. At the selected conditions differential pulse voltammetric responses had good linear relationship with luteolin concentration from 5.0×10^{-8} to 5.0×10^{-5} mol L⁻¹ and the detection limit was 7.59×10^{-9} mol L⁻¹. The Duiwei soft capsules sample was successfully detected by the proposed method.

Keywords: Three-dimensional graphene, Gold nanoparticle, Luteolin, Carbon ionic liquid electrode, Electroanalysis

1. INTRODUCTION

Luteolin belongs to flavonoids drug that is abundant in various plants including celery, green pepper, parsley and perilla leaf [1]. It has been reported that luteolin exhibits many pharmacological functions including anti-oxidation, anti-bacteria, anti-virus, anti-inflammatory and anti-carcinogenic effects [2]. Recent publications indicate that luteolin exhibits excellent anti-proliferative activity to cancer cells and suppresses the oxidation injure to biomolecules such as DNA, lipid or proteins [3, 4]. Various analytical techniques including HPLC [5], capillary electrophoresis [6], gas chromatography

[7], spectrophotometry [8] and electroanalysis [9] have been published for luteolin analysis. However some of them need complicated equipments, time-consuming procedure, cost reagents or insufficient selectivity. In the molecular structure of luteolin, catechol group is present on the B ring, which is electroactive and electrochemical behaviors of luteolin have been investigated on various modified electrodes [10]. Zhao et al. applied a multi-walled carbon nanotube modified electrode for voltammetric analysis of luteolin in peanut hulls [11]. Zeng et al. used a macroporous carbon modified electrode for luteolin analysis [12]. Pang et al. constructed a graphene (GR) and hydroxyapatite nanocomposite modified electrode for luteolin detection [13]. Sun et al. fabricated a GR modified electrode for the voltammetric detection of luteolin [14].

GR is a carbon nanosheet that shows great promise in sensing field due to its high specific surface area, unique planar structure and fast electron transfer conductivity, which is often applied to electrochemical sensor [15]. However the aggregation between GR nanosheet results in the decrease of performances. In recent years three-dimensional (3D) GR has been investigated because of the porous structure with large surface area [16]. Various methods are devised for 3DGR synthesis, including chemical vacuum deposition, template, sol-gel and electrodeposition [17]. Du et al. used a 3D functionalized GR for simultaneous determination of hydroquinone and catechol [18]. Sun et al. fabricated a 3DGR based electrode for direct electrochemistry of redox proteins [19]. To modulate the interfacial properties, 3DGR based composite has been synthesized [20]. Gold nanoparticles (AuNPs) exhibit the advantages including high conductivity, enhanced catalytic activity and good biocompatibility [21], which have been used in electrochemical sensor. For example direct electrochemistry of redox proteins had been realized on nanosized Au and GR modified electrode [22, 23].

In this paper AuNPs and 3DGR were electrodeposited on carbon ionic liquid electrode (CILE), which was used for investigation on voltammetric behaviors of luteolin. CILE is prepared by using ionic liquid N-hexylpyridinium hexafluorophosphate (HPPF₆) as the modifier in the traditional carbon paste electrode. At the optimal procedure a pair of well-defined redox peak of luteolin could be observed on cyclic voltammetric curves, which indicated that electrochemical reaction of luteolin was realized. The results were due to the presence of Au/3DGR composite that could adsorb more luteolin on the electrode surface with the electron transfer rate accelerated. Then a new method was established for luteolin and its related drug samples analysis.

2. EXPERIMENTAL

2.1. Instruments and reagents

Electrochemical measurements were performed on a CHI 660D electrochemical analyzer (Shanghai CH Instrument, China) with a three-electrode cell. Au/3DGR/CILE was acted as the working electrode with a platinum wire auxiliary electrode and a saturated calomel reference electrode (SCE). Scanning electron microscopy (SEM) was conducted with a JSM-7100F scanning electron microscope (JEOL, Japan).

HPPF₆ (Lanzhou Yulu Fine Chem. Co., China), graphene oxide (GO, Taiyuan Tanmei Co., China), graphite powder (average particle size 30 μm, Shanghai Colloid Chem. Plant, China) and chloroauric acid (HAuCl₄, Shanghai Chem. Plant, China) were used as received. The stocking solution of luteolin (1.0 mmol L⁻¹, Xi'an Yuquan Biotechnology Ltd. Co., China) was prepared with anhydrous ethanol. 0.04 mol L⁻¹ Britton-Robinson (B-R) buffer solution was used as the supporting electrolyte with doubly distilled water used throughout.

2.2. Preparation of the modified electrode

CILE was prepared with graphite powder and HPPF₆ based on the reference [24], which was polished on the weighing paper before use. The formation of 3DGR was performed with the potentiostatic method in a 3.0 mg mL⁻¹ GO solution and 0.15 mol L⁻¹ LiClO₄ solution with magnetic stirring and N₂ bubbling [25]. Then electrochemical reduction was performed at -1.3 V for 600 s to obtain 3DGR/CILE. After rinsed with water and dried in air, AuNPs were further electrodeposited with a 5.0 mmol L⁻¹ HAuCl₄ and 0.5 mol L⁻¹ KNO₃ mixture solution at -0.4 V for 300 s. The Au/3DGR/CILE was cleaned with water and dried before use.

2.3. Electrochemical detection

The standard or sample solution was mixed with 0.04 mol L⁻¹ B-R buffer (pH 4.0). Cyclic voltammetry was scanned from 0.1 to 0.8 V at the scan rate of 0.1 V s⁻¹. Differential pulse voltammetry was recorded from 0.2 to 0.65 V with pulse amplitude as 50 mV, pulse width as 50 ms and pulse period as 0.2 s.

3. RESULTS AND DISCUSSION

3.1. Characteristics of the modified electrode

The images of 3DGR and Au/3DGR on CILE surface were recorded with the SEM results shown in Fig. 1. It can be seen that 3DGR had a porous network with layered structure and large surface area (Fig.1A). After electrodeposition of AuNPs, the surface became rougher with many AuNPs present on the surface of GR nanosheet (Fig.1B), which greatly increased the effective surface area. Electrochemical impedance spectroscopy (EIS) is often used to check the impedance changes during the modification. The electron transfer resistance (Ret) depends on the dielectric and insulating features at the electrode/electrolyte interface. As shown in Fig. 1 C, Ret results of CILE, 3DGR/CILE, Au/CILE and Au/3DGR/CILE were got as 71.8 Ω, 24.7 Ω, 17.8 Ω and 8.5 Ω. The gradually decrease of the Ret data proved that the surface resistance was decreased, which was ascribed to the existence of high conductive 3DGR, AuNPs and their synergistic effects. GR nanosheet and AuNPs have been reported to exhibit excellent conductivity, which can be used to fast the electron transfer rate and decrease the interfacial resistance [26, 27].

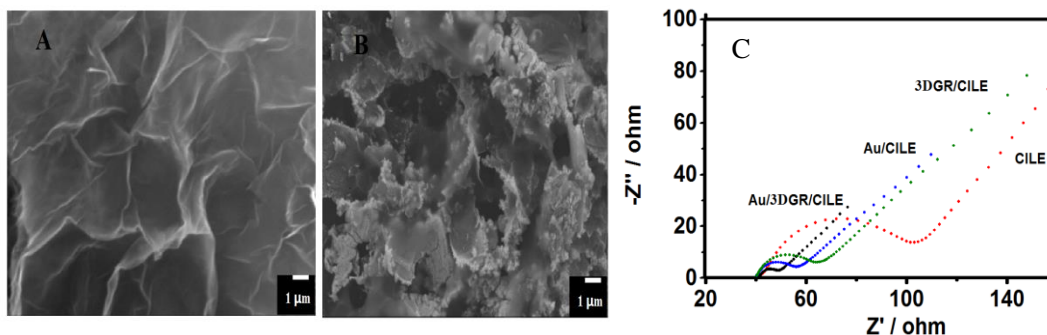


Figure 1. SEM images of (A) 3DGR/CILE and (B) Au/3DGR/CILE, (C) EIS of different modified electrodes in a $10.0 \text{ mmol L}^{-1} [\text{Fe}(\text{CN})_6]^{3-/4-}$ and $0.1 \text{ mol L}^{-1} \text{ KCl}$ solution with the frequencies swept from 10^5 to 1 Hz.

3.2. Cyclic voltammetric behaviors of luteolin

Voltammetric behavior of luteolin on different electrodes was checked by cyclic voltammetry with the curves shown in Fig. 2. On all the electrodes a pair of redox peaks could be observed with the currents became bigger gradually along with the modification of AuNPs and GR on the electrode. The phenomenon was the typical electrochemical response of luteolin due to its electroactive group [28]. On CILE the smallest redox peak currents could be observed and the currents increased on Au/CILE and 3DGR/CILE. The results were ascribed to the presence of AuNPs or 3DGR on CILE surface that exhibited excellent performance with certain electrocatalytic activity, which were the typical behaviors of nanomaterials modified electrodes. On Au/3DGR/CILE the biggest peak currents were got with the smallest peak-to-peak separation (ΔE_p) of 59 mV, and the ratio of anodic to cathodic peak currents (I_{pa}/I_{pc}) was approximately to 1.0. Therefore a reversible electrochemical process took place on the modified electrodes due to the synergistic functions of AuNPs and 3DGR, including porous structure with large surface area and high electrical conductivity that promoted electron transfer rate.

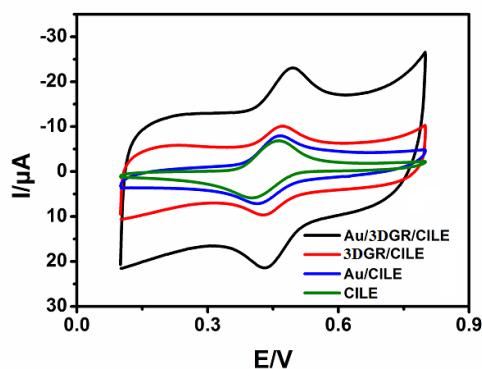


Figure 2. Cyclic voltammograms of $1.0 \text{ } \mu\text{mol L}^{-1}$ luteolin on different modified electrodes with scan rate as 100 mV s^{-1} (from the inner to the outer: CILE, Au/CILE, 3DGR/CILE, Au/3DGR/CILE).

3.3. Electrochemical investigation

The effect of buffer pH on the voltammetric response of $1.0 \mu\text{mol L}^{-1}$ luteolin on Au/3DGR/CILE was checked from 1.5 to 7.0. Along with the increase of the buffer pH cyclic voltammograms deformed gradually, showing that electrode reaction process became slowly. The formal peak potential ($E^{0'}$) shifted negatively with buffer pH, indicating that protons took part in the electrochemical reaction. The relationship of $E^{0'}$ with pH was plotted and the linear regression equation was $E^{0'}(\text{V}) = -0.061 \text{ pH} + 0.72$ ($\gamma = 0.999$). The slope (-61.0 mV pH^{-1}) was close to the theoretical value (-59.0 mV pH^{-1}), therefore the number of protons and electrons involved in electrochemical reaction was same [29]. The largest redox peak current appeared at pH 4.0 buffer solution, which was selected for the voltammetric investigation. In the acidic buffer solution enough protons could be provided for the electrochemical reaction of luteolin, then the electrochemical reaction of luteolin was easy to be realized in the acidic solution.

The influence of scan rate on cyclic voltammetric response of $1.0 \mu\text{mol L}^{-1}$ luteolin was investigated on Au/3DGR/CILE in pH 4.0 B-R buffer and the curves were shown in Fig. 3. From 20 to 500 mV s^{-1} the peak currents increased gradually with scan rate. The linear relationships of I_p with v was calculated as $I_{pa}(\mu\text{A}) = -0.12 - 32.93v$ (V s^{-1}) ($\gamma = 0.999$) and $I_{pc}(\mu\text{A}) = -0.32 - 27.89v$ (V s^{-1}) ($\gamma = 0.999$), which belonged to an adsorption-controlled electrochemical process [30]. Therefore the presence of Au/3DGR nanocomposite on the electrode had a large surface area for the adsorption of luteolin, which could increase the surface concentration of luteolin with the increase of the sensitivity.

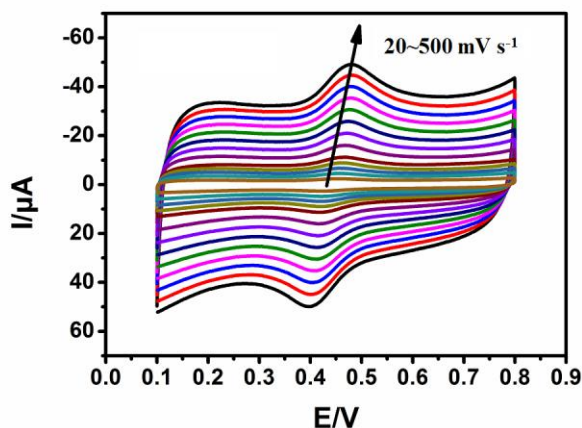
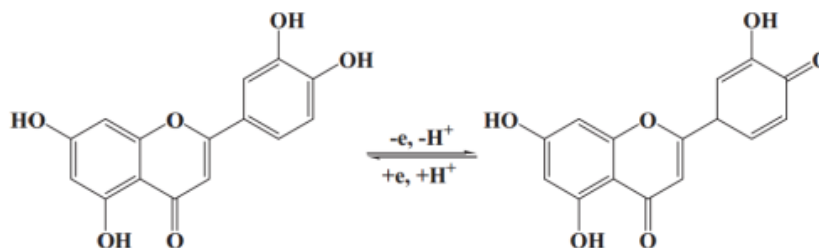


Figure 3. Cyclic voltammograms of $1.0 \mu\text{mol L}^{-1}$ luteolin on Au/3DGR/CILE in pH 4.0 B-R buffer at various scan rates (20, 40, 60, 80, 100, 150, 200, 300, 400, 500 mV s^{-1})

As shown in Fig.3 the increase of scan rate also resulted in the increase of the peak-to-peak separation (ΔE_p), which indicated a quasi-reversible electrode process. Then the relationship of the peak potentials with $\ln v$ were calculated with regression equations as $E_{pa}(\text{V}) = 0.050 \ln v(\text{V s}^{-1}) + 0.49$ ($\gamma = 0.997$) and $E_{pc}(\text{V}) = -0.045 \ln v(\text{V s}^{-1}) + 0.041$ ($\gamma = 0.997$). According to Laviron's equation [31], electrochemical parameters were got with the charge transfer coefficient (α) as 0.53, the apparent heterogeneous electron transfer rate constant (k_s) as 1.01 s^{-1} and the electron transfer number (n) as

0.95. Because the number of proton and electron involved in the electrode reaction was the same, then one proton was involved in the electrode reaction. Therefore the electrochemical reaction of luteolin could be expressed as scheme 1, which involved the oxidation of 4'-hydroxyl on the benzene ring with one electron and one proton on the forward process and reduced at the backward scan [32].



Scheme 1. Electrochemical reaction process of luteolin

3.4. Calibration curve

At the optimal conditions luteolin standard solutions at different concentration were scanned by differential pulse voltammetry with the typical curves shown in Fig. 4A. The oxidation peak currents increased with luteolin concentration from $0.05 \mu\text{mol L}^{-1}$ to $50.0 \mu\text{mol L}^{-1}$. As shown in Fig. 4B, the linear regression equation was $I_{pa}(\mu\text{A}) = 10.14 C(\mu\text{mol/L}) + 2.437$ ($\gamma=0.983$). The detection limit was estimated to be 7.59 nmol L^{-1} ($3S_0/S$), where 3 is the factor at the 99% confidential level, S_0 is the standard deviation of the blank measurements without luteolin ($n = 9$) and S is the slope value of the calibration curve. The analytical parameters for the electrochemical detection of luteolin by different kinds of modified electrodes were summarized in table 1. On Au/3DGR/CILE a wider detection range and lower detection limit could be achieved with good sensitivity.

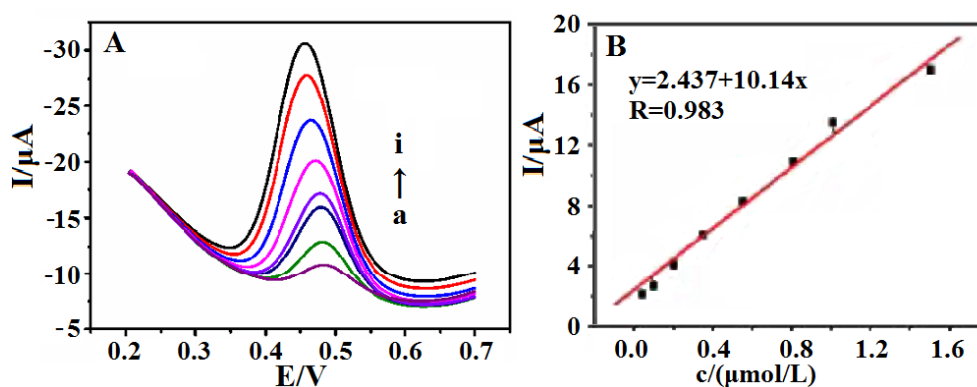


Figure 4. (A) DPV curves of different luteolin concentration on Au/3DGR/CILE in 0.04 mol L^{-1} pH 4.0 B-R buffer (from a to i: $0.05, 0.1, 0.2, 0.35, 0.55, 0.8, 0.1, 1.5 \mu\text{mol L}^{-1}$); (B) linear relationship of the oxidation peak current with the luteolin concentration.

Table 1. Comparison of the analytical parameters for electrochemical detection of luteolin.

Electrode	Linear range (mol L ⁻¹)	Detection limit (mol L ⁻¹)	Reference
MWNTs/GCE	2.0×10^{-10} - 3.0×10^{-9}	6.0×10^{-11}	11
MPC/GCE	3.0×10^{-7} - 3.0×10^{-5}	1.3×10^{-9}	12
GNs/HA/GCE	2.0×10^{-8} - 1.0×10^{-5}	1.0×10^{-8}	13
CS-GR/GCE	2.0×10^{-9} - 6.0×10^{-5}	5.93×10^{-10}	14
GCE	1.0×10^{-8} - 1.0×10^{-6}	5.0×10^{-9}	28
HPLDE	4.0×10^{-9} - 1.0×10^{-6}	1.0×10^{-9}	33
Au-BMIPF ₆ -CPE	1.0×10^{-7} - 5.8×10^{-6}	2.8×10^{-8}	34
Au/3DGR/CILE	5.0×10^{-8} - 5.0×10^{-5}	7.59×10^{-9}	this work

MWCNT: Multi-walled carbon nanotubes, GCE: Glassy carbon electrode, MPC: Macroporous carbon, GN: Graphene, HA: Hydroxyapatite, CS: Chitosan, HPLDE: Heated pencil lead disk electrode, BMIPF₆: 1-butyl-3-methylimidazolium hexafluorophosphate, CPE: carbon paste electrode.

3.5. Interference

The influences of other substances on analysis of $1.0 \mu\text{mol L}^{-1}$ luteolin were checked with the data listed in table 2, which was performed by the addition of these substances in luteolin standard solution. Then the voltammetric responses were recorded and the changes were calculated. As shown in table 2 few of them influenced the analysis with the relative errors less than $\pm 5\%$, therefore the proposed method had good selectivity for luteolin detection.

Table 2. Influence of coexisting substances on the detection of $1.0 \mu\text{mol L}^{-1}$ luteolin (n=3)

Coexisting Substances	Concentration ($\mu\text{mol L}^{-1}$)	Relative error (%)	Coexisting substances	Concentration ($\mu\text{mol L}^{-1}$)	Relative error (%)
L-Threonine	100.0	2.12	L-Proline	100.0	4.31
L-Arginine	100.0	2.17	Ni ²⁺	100.0	1.29
L-Cystine	100.0	3.25	Ba ²⁺	100.0	2.43
L-Alanine	100.0	1.38	Ca ²⁺	100.0	3.17
L-Leucine	100.0	1.71	K ⁺	100.0	2.28
L-Tryptophane	100.0	1.82	Na ²⁺	100.0	3.81
L-Lysine	100.0	3.67	Cr ³⁺	100.0	2.14

3.6. Stability and reproducibility

The reproducibility of Au/3DGR/CILE was evaluated by four-time detections of a luteolin solution ($1.0 \mu\text{mol L}^{-1}$) and the relative standard deviation (RSD) was 3.0%. The stability of Au/3DGR/CILE was checked by 40 cyclic scanning in pH 4.0 B-R buffer and the background current

kept unchanged. The long-term stability of Au/3DGR/CILE was tested by storing at room temperature for 10 days and the oxidation current of luteolin was about 90% of its initial data. These results demonstrated that Au/3DGR/CILE had good stability and reproducibility for electrochemical application.

3.7. Analytical application

The luteolin content in Duiyiwei soft capsules (Gansu Duiyiwei pharmaceutical Ltd. Co., Z10970053) was determined by Au/3DGR/CILE. Five soft capsules were finely pulverized with the powder dissolved with ethanol. After sonicated for 0.5 hours and refluxed for 2 hours, the turbid liquid was filtered with the clear filtrate diluted by pH 4.0 B-R buffer solution to prepare the sample solution. Then the sample solution was detected by the procedure with the content calculated as $9.43 \mu\text{mol L}^{-1}$. The recovery was calculated by the addition of the standard luteolin solution with the values obtained from 95.28 to 103.77%. Therefore the proposed method was able to use for the luteolin content analysis in the Duiyiwei soft capsules.

4. CONCLUSION

Electrodeposition of 3DGR and AuNPs were realized on the surface of CILE to get an Au/3DGR nanocomposite modified electrode with excellent electrochemical performance. Electrochemistry of luteolin was realized and enhanced on Au/3DGR/CILE with electrochemical parameters calculated. This modified electrode was further used for the sensitive analysis of luteolin content in Duiyiwei soft capsules. The result proved that Au/3DGR nanocomposite modified electrode was suitable for the drug analysis with the advantages including faster response, wider linear and lower detection limit.

ACKNOWLEDGEMENTS

The financial support of this project by the Program for Innovative Research Team in University (IRT-16R19), the Science and Research Key Project of Universities of Hainan Province (Hnky2016ZD-10), and the Natural Science Foundation of Hainan Province (20162031).

References

1. L. E. Craker and J. E. Simon, *Herbs, spices and medicinal plants: recent advances in botany, horticulture and pharmacology*, Oryx Press, (1986).
2. H. Kikuzaki, M. Hisamoto, K. Hirose, K. Akiyama and H. Taniguchi, *J. Agr. Food Chem.*, 50 (2002) 2161.
3. L. Fu, B. T. Xu, X. R. Xu, R. Y. Gan, Y. Zhang, E. Q. Xia and H. B. Li, *Food Chem.*, 129 (2011) 345.
4. P. Knekt, R. Jarvinen, A. Reunanen and J. Maatela, *Bmj-Brit. Med. J.*, 312 (1996) 478.
5. Y. Z. Zhou, X. X. Liu, X. H. Zheng and J. B. Zheng, *Chromatographia*, 66 (2007) 635.

6. Y. Y. Li, Q. F. Zhang, H. Y. Sun, N. K. Cheung and H. Y. Cheung, *Talanta*, 105 (2013) 393.
7. C. S. Liu, Y. S. Song, K. J. Zhang, J. C. Ryu, M. Kim and T. H. Zhou, *J. Pharmaceut. Biomed. Anal.*, 13 (1995) 1409.
8. I. Baranowska and D. Raróg, *Talanta*, 55 (2001) 209.
9. M. Filipiak, *Anal. Sci.*, 17 (2001) 1667.
10. L. V. Jørgensen, H. L. Madsen, M. K. Thomsen, L. O. Dragsted and L. H. Skibsted, *Free Radical Res.*, 30 (1999) 207.
11. D. M. Zhao, X. H. Zhang, L. J. Feng and S. F. Wang, *Food Chem.*, 127 (2011) 694.
12. L. J. Zeng, Y. F. Zhang, H. Wang and L. P. Guo, *Anal. Methods*, 5 (2013) 3365.
13. P. F. Pang, Y. P. Liu, Y. L. Zhang Y. T. Gao and Q. F. Hu, *Sensor. Actuat. B-Chem.*, 194 (2014) 397.
14. G. J. Li, L. H. Liu, Y. Cheng, S. X. Gong, X. L. Wang, X. J. Geng and W. Sun, *Anal. Methods*, 6 (2014) 9354.
15. E. B. Bahadır and M. K. Sezginürk, *Trac-Trend. Anal. Chem.*, 76 (2016) 1.
16. C. Li and G. Q. Shi, *Nanoscale*, 4 (2012) 5549.
17. L. L. Jiang and Z. J. Fan, *Nanoscale*, 6 (2014) 1922.
18. J. Du, L. L. Ma, D. L. Shan and X. Q. Lu, *J. Electroanal. Chem.*, 722 (2013) 38.
19. W. Sun, F. Hou, S. X. Gong, L. Han, W. C. Wang, F. Shi, J. W. Xi, X. L. Wang and G. J. Li, *Sensor. Actuat. B-Chem.*, 219 (2015) 331.
20. P. T. Xu, J. X. Yang, K. S. Wang, Z. Zhou and P. W. Shen, *Chinese Sci. Bull.*, 57 (2012) 2948.
21. G. M. Zhang, *Nanotechnol. Rev.*, 2 (2013) 269.
22. G. N. Li, T. T. Li, Y. Deng, Y. Cheng, F. Shi, W. Sun and Z. F. Sun, *J. Solid State Electr.*, 17 (2013) 2333.
23. F. Shi, J. W. Xi, F. Hou, L. Han, G. J. Li, S. X. Gong, C. X. Chen and W. Sun, *Mat. Sci. Eng. C-Mater.*, 58 (2016) 450.
24. W. Sun, Y. Y. Duan, Y. Z. Li, T. R. Zhan and K. Jiao, *Electroanal.*, 21 (2009) 2667.
25. K. X. Sheng, Y. Q. Sun, C. Li, W. J. Yuan and G. Q. Shi, *Sci. Rep.*, 2 (2012) 247.
26. Y. Song, Y. Luo, C. Zhu, H. Li, D. Du, Y. Lin, *Biosens. Bioelectron.*, 76 (2016) 195.
27. K. Saha, S. S. Agasti, C. Kim, X. Li, V. M. Rotello, *Chem. Rev.*, 112 (2012) 2739.
28. A. L. Liu, S. B. Zhang, L. Y. Huang, Y. Y. Cao, H. Yao and W. Chen, *Chem. Pharm. Bull.*, 56 (2008) 745.
29. A. J. Bard and L. R. Faulkner, *Electrochemical methods: fundamentals and applications*, Wiley, New York, (1980).
30. J. Wang, *Analytical Electrochemistry*, 2nd ed., Wiley, New York, (2000).
31. E. Laviron, *J. Electroanal. Chem.*, 101 (1979) 19.
32. J. Kang, X. Lu, H. Zeng, H. Liu and B. Lu, *Anal. Lett.*, 35 (2002) 677.
33. S. H. Wu, S. H. Wu, B. J. Zhu, Z. X. Huang and J. J. Sun, *Electrochem. Commun.*, 28 (2013) 47.
34. A. C. Franzoi, I. C. Vieira, J. Dupont, C. W. Scheeren and L. F. de Oliveira, *Analyst*, 134 (2009) 2320.